Depropagation Kinetics of Sterically Demanding Monomers: A Pulsed Laser Size Exclusion Chromatography Study

Zachary Szablan, Martina H. Stenzel, Thomas P. Davis, Leonie Barner, and Christopher Barner-Kowollik*

Centre for Advanced Macromolecular Design, School of Chemical Engineering and Industrial Chemistry, The University of New South Wales, Sydney, NSW 2052, Australia

Received March 2, 2005; Revised Manuscript Received May 6, 2005

ABSTRACT: Conventional pulsed laser polymerization coupled with size exclusion chromatography (PLP−SEC) as well as multipulse pulsed laser polymerization has been employed to study the depropagation kinetics of the sterically demanding 1,1-disubstituted monomers dicyclohexyl itaconate (DCHI), dibutyl itaconate (DBI), and dimethyl itaconate (DMI). The effective rate coefficient of propagation, k_p^{eff}, was determined in bulk and solution of cyclohexanone (DCHI) and *N*-methylformamide (DMI) for monomer concentrations between $1.5 < c_M^0 < 7.1$ mol L^{-1} in the temperature range $0 < T < 90$ °C. The resulting Arrhenius plots (i.e., ln k_p^{eff} vs $1/RT$) displayed a significant curvature in the higher temperature regimes and were analyzed in their respective linear parts to yield the activation parameters of the forward reaction. In the temperature region where no depropagation was observed, the following set of Arrhenius parameters for k_p were obtained for the bulk systems: DCHI ($E_p = 26.5$ kJ mol^{-1}, ln A_p/L mol^{-1} s^{-1} = 11.5), DBI ($E_p = 21.3$ kJ mol^{-1}, ln A_p/L mol^{-1} s^{-1} = 10.4), DMI ($E_p = 27.8$ kJ mol^{-1}, ln A_p/L mol^{-1} s^{-1} = 13.5). In addition, the k_p^{eff} data were analyzed in the depropagation regime for DCHI, resulting in estimates for the associated enthalpy and entropy ($\Delta H = -53.5$ kJ mol^{-1} and $\Delta S = -142.3$ J mol^{-1} K^{-1}) of polymerization. The value for the heat of polymerization was independently measured via on-line differential scanning calorimetry (DSC) as well ($\Delta H = -55.0$ kJ mol^{-1}). ΔH of DBI and DMI were also determined via DSC or are available in the literature ($\Delta H = -42.0$ and -60.5 kJ mol^{-1}). These numbers were used to determine the respective entropies of polymerization for both monomers ($\Delta S = -110$ and -156 J mol^{-1} K^{-1}) by a fitting procedure of the k_p^{eff} data. DBI polymerization displays significantly different activation parameters as well as thermodynamic properties in comparison with the corresponding DCHI and DMI polymerizations. With decreasing monomer concentration, it is increasingly more difficult to obtain well-structured molecular weight distributions. The DCHI system displayed a significant reduction in k_p^{eff} with increasing cyclohexanone concentration.

Introduction

Our interest in sterically demanding monomers is prompted by the realization that such monomers may be employed to generate block copolymers of approximate rod/coil structure using living free radical polymerization methodologies (i.e., the CSIRO invented reversible addition−fragmentation chain transfer (RAFT)[1] process).[2] Of interest for the formation of such rod/coil structures is the itaconate class of monomers, e.g., dicyclohexyl itaconate (DCHI), dibutyl itaconate (DBI), and dimethyl itaconate (DMI) (see structural images depicted in Scheme 1).

A wide array of hindered monomer systems have been studied via electron spin resonance (ESR) spectroscopy (in conjunction with steady-state polymerization rate measurements) with the aim of deducing propagation, k_p, and termination rate, k_t, coefficients.[3−6] Macromolecules produced from hindered monomers can display unique chain properties. Previous studies have shown that hindered monomers, unlike other monomers, may not show a pronounced chain length dependence of the termination reaction. It may also be possible that the chain length dependence of k_p observed in varying degrees for some monomers is less pronounced in hindered monomer systems. Such observations indicate that the sterically demanding cyclohexyl substituents in e.g. DCHI lead to the macromolecule arranging itself into stiff and straight rods,[7] confirming observations made by Otsu and co-workers in 1985.[8] The property of chain stiffness opens the door for the above-mentioned relatively facile synthesis of a range of rod/coil block copolymers via the combination of an itaconate-based polymer block followed by a block of a conventional monomer such as styrene. A first step toward the application and design of itaconate-based rod/coil block copolymers (with *p*styrene as the second block) was discussed in an earlier publication, in which we reported the successful controlled free radical polymerization of DCHI and DBI via the RAFT process.[2] The inherent difference in ceiling temperatures between the coil (T_c(styrene, bulk) = 310 °C)[9] and the rod part of the generated copolymers may allow for a targeted depolymerization of the rod component in a cast polymer film (where the block copolymer has undergone phase sepa-

Scheme 1. Sterically Demanding Monomers Dicyclohexyl Itaconate (DCHI), Dibutyl Itaconate (DBI), and Dimethyl Itaconate (DMI) Used for the Depropagation Study

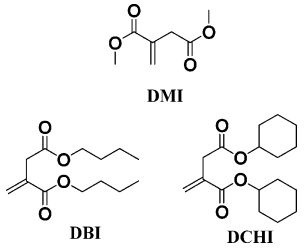

* Corresponding author. E-mail: camd@unsw.edu.au.

10.1021/ma050444l CCC: $30.25
Published on Web 06/15/2005

ration) and the subsequent formation of macromolecular imprints. (The rod part should have a T_c significantly lower than the coil part, ideally in the region of 60−100 °C.) Thus, our study into the depolymerization kinetics of these polymers is partly driven by the potential application of the associated block copolymers for the generation of macromolecular imprints.[2]

The monomers examined in the present contribution represent varying degrees of steric bulk, increasing from dimethyl itaconate (DMI) to dibutyl itaconate (DBI) and dicyclohexyl itaconate (DCHI). These itaconate species are also referred to as "hindered monomers". This term is imparted to the itaconate class due to the bulky substituent groups that can cause extremely slow propagation and termination rates. The bulky groups in the vicinity of the vinyl functionality prevent the propagating radical from effectively reacting with monomer, so that the propagation rate, k_p, and termination rate coefficient, k_t, are significantly lower than those of more common monomer systems under comparable reaction conditions (e.g., k_p(methyl acrylate, 60 °C) = 27 000 L mol^{-1} s^{-1}, $\langle k_t \rangle$(methyl acrylate, 60 °C) = 1 × 10^8 L mol^{-1} s^{-1}, k_p(DCHI, 60 °C) = 6.8 L mol^{-1} s^{-1}, $\langle k_t \rangle$(DCHI, 60 °C) = 1403 L mol^{-1} s^{-1}).[10−14]

The determination of the propagation rate coefficients is today routinely carried out by the IUPAC recommended pulsed laser polymerization (PLP) technique.[15,16] This methodology—in which the resulting polymeric material is analyzed via size exclusion chromatography (SEC)—allows for the accurate determination of the propagation rate coefficient k_p. Our group has previously published values for the propagation rate coefficents[13,14,17] and termination rate coefficients[12,13] of both DMI and DCHI using the PLP−SEC technique. These studies show in detail that the PLP−SEC method is capable of determining rate coefficients of hindered monomers, albeit with some modifications (see below).

In the case of many monosubstituted ethylene-type monomers other side reactions (such as potentially excessive transfer to monomer) become dominant well before the ceiling temperature is reached.[18] However, for some 1,1-disubstituted ethylene monomers (such as α-methylstyrene[19]) it is possible to polymerize at reaction conditions where the effects of the reverse reaction cannot be neglected.[20] Understanding depropagation for hindered monomers systems and its associated effects on the polymer molecular weight are necessary to ensure a uniform polymer product and—more important in the context of macromolecular imprints—allow for the selection of reaction conditions where depropagation dominates. Furthermore, hindered monomer systems are potentially attractive candidates for investigations into chain length dependent termination rate coefficients via stationary RAFT experiments.[21−23] Information about their behavior at higher temperatures is paramount for a successful application of the RAFT-CLD-T (i.e., RAFT chain length dependent termination) methodology for mapping out chain length dependent k_t. Thus, the focus of the present contribution is the determination of reaction conditions in which depolymerization becomes prominent and to obtain (when possible) an estimation of the ceiling temperature (T_c[24]) for the aforementioned monomers via conventional and the so-called multipulse pulsed laser polymerization techniques.

Multipulse Initiation in PLP. The laser-induced increase in termination processes under PLP conditions is the underpinning mechanism that causes the characteristic peaks that occur in the resulting chain length distribution. These characteristic peaks reflect an increased termination probability of the growing chain at the moment of a laser flash as a result of the formation of a large free radical population. The evaluation of these peaks is the basis for the calculation of the effective propagation rate coefficient k_p^{eff} according to eq 1

$$L_i = k_{p,i}^{eff}[M]t_0 \quad (1)$$

where L_i is the kinetically relevant chain length obtained from either the first ($i = 1$) or second ($i = 2$) inflection point preceding a maximum of the distribution and t_0 is the time between successive laser pulses. At the end of t_0, when the subsequent laser pulse irradiates the sample, the remaining radicals are exposed to the newly generated radicals, leading to a great increase in the probability of their termination. The termination of the growing radical species occurs at a chain length close to L_i. The best estimate for L_i is (in the majority of cases) the inflection point of the PLP controlled peak of the polymer molecular weight distribution (MWD) (see for example refs 15, 25, and 26) which corresponds to the peaks of the derivative function of the PLP controlled MWD. Self-consistent PLP is obtained when well-resolved additional peaks in the resulting molecular weight distribution are observed. Pseudo-stationary pulsed laser polymerization theory[27] implies that the shape of the distribution is governed by the dimensionless product, C, of the radical concentration, ρ, the termination rate coefficient, and the dark time, t_0 (see for example ref 28 for a detailed description of the underpinning theory of PLP−SEC). Typical values of C are between 0.5 and 10, with higher C values yielding more pronounced first additional peaks. Hindered monomers are characterized by low termination rate coefficients; therefore, the product of ρ and t_0 has to be high in order to obtain well-structured distributions. This can be achieved by increasing laser power and initiator concentration or increasing dark time between successive laser pulses. However, there are experimental limitations to implementing this theory, and these are discussed in a previous publication by our group.[13]

The most feasible and promising method to increase the value of the product C and thus obtain well-structured MWDs is achieved by increasing ρ by applying several pulses over a very short time interval. The extremely low propagation rate coefficients for the monomers studied in the present work make negligible the uncertainty caused by the extension of the initiation period from 20 ns (conventional PLP) up to 1.5 s in this work. A burst of n pulses within 1 s leads to a free radical concentration n times higher as in normal PLP, inaccessible using conventional PLP. For example, we have noticed that considerable improvement can be achieved in the resulting MWD obtained during the polymerization of DBI using the multipulse technique. Olaj and Zifferer[29] have shown in great detail via simulations that arbitrary periodic initiation profiles (even with discontinuities) lead to MWDs with additional peaks and that yield reliable values for k_p.

We have previously used the classical and multipulse PLP−SEC technique successfully to measure k_p values between 20 and 50 °C for both dimethyl itaconate[14] and dicyclohexyl itaconate,[13] respectively. In both previous

publications, reaction conditions were such that depolymerization did not occur ($k_p^{eff} = k_p$). Therefore, the experimental values and Arrhenius parameters reported for these monomers correspond to the forward reaction rate coefficients defined by eq 1. The present study extends the temperature range under investigation, giving access to k_p^{eff} at both lower and higher temperatures ($0 < T < 90$ °C) and at reduced monomer concentration in solution of cyclohexanone and *N*-methylformamide as well as incorporating the complete study of a new hindered itaconate monomer, which may sterically lie between the two itaconate species previously studied.

Within the present study the effect of depropagation on the generated MWDs in multipulse PLP was also investigated via the PREDICI simulation package on the example of DCHI. This monomer was selected for the theoretical investigation since most of the relevant kinetic parameters (including reliable termination rate coefficients) are available.

Propagation/Depropagation Reaction Kinetics. For every monomeric species undergoing chain polymerization there is a temperature at which the reverse reaction, depolymerization, can no longer be considered insignificant. The propagation step is thus reversible, although often considered irreversible, and thus a thermodynamic equilibrium can be attained (see ref 28 and the literature cited therein for a description of the theoretical background) While we wish to employ depropagation approaches (in the long term) to achieve macromolecular imprints, depolymerization can also be used to achieve molecular weight control in certain copolymerization systems.[30] The thermodynamic equilibrium associated with depolymerization can be described by the magnitude of the free energy difference, ΔG, between the polymer and the monomer (eq 2)

$$\Delta G = \Delta H - T\Delta S \tag{2}$$

and is thermodynamically favored when ΔG is negative. The heat of polymerization, ΔH, of all (viable) free radical polymerizations is negative with values typically in the range of -30 to -80 kJ mol^{-1}.[31] Free radical polymerization entropies are also typically negative in the range -100 to -120 J K^{-1} mol^{-1}.[31] Thus, under low-temperature conditions, the exothermicity of the reaction exceeds the entropic term and ΔG is negative. At elevated temperatures, the entropic term becomes significantly larger until the enthalpic and entropic terms are equal. The temperature at which $T\Delta S = \Delta H$ is the temperature where $\Delta G = 0$ and propagation and depropagation display identical rates (no net polymerization). This temperature is known as the ceiling temperature of the polymer and is denoted T_c.[24] The kinetic interpretation of the propagation and depropagation effects is described by eqs 3 and 4, respectively.

$$R_i^{\bullet} + M \xrightarrow{k_p} R_{i+1}^{\bullet} \tag{3}$$

$$R_{i+1}^{\bullet} \xrightarrow{k_{dp}} R_i^{\bullet} + M \tag{4}$$

where R_i represents the growing radical of length i and M the monomer, k_p denotes the propagation rate coefficient and k_{dp} the depropagation rate coefficient. The depropagation process results in a lowering of the rate of polymerization, R_p, according to eq 5

$$R_p = k_p[M][R^{\bullet}] - k_{dp}[R^{\bullet}] = \left(k_p - \frac{k_{dp}}{[M]}\right)[M][R^{\bullet}] = k_p^{eff}[M][R^{\bullet}] \tag{5}$$

where k_p^{eff} is the effective rate coefficient of propagation defined by eq 6:

$$k_p^{eff} = k_p - \frac{k_{dp}}{[M]} \tag{6}$$

The depropagation effect is therefore inversely proportional to the monomer concentration. Understanding and consequently being able to model the effects of depropagation are necessary for the development of uniform polymeric products, especially in the case of living/controlled polymerizations such as the RAFT process. To model polymerization processes at temperatures where depropagation becomes relevant, the depropagation kinetics of the species must be known. The depropagation kinetics are governed by the enthalpy, ΔH, and entropy, ΔS, of the polymerizing monomer and can be rationalized as depicted below.

$$\Delta H = E_p - E_{dp} \tag{7}$$

$$\Delta S = R \ln(A_p/A_{dp}) + R \ln[M] \tag{8}$$

$$k_p = A_p \exp(-E_p/RT) \tag{9}$$

$$k_{dp} = A_{dp} \exp(-E_{dp}/RT) \tag{10}$$

where E and A are the activation energies of the forward (subscript p) and reverse (subscript dp) rate reactions as expressed in the usual Arrhenius form. To our knowledge, the only published data for the enthalpies of polymerization of any of the monomers considered in the present study is for DMI by Dainton et al., who determined (via reaction calorimetry) an enthalpy, ΔH, of 60.5 kJ mol^{-1} at 27 °C.[32] To our knowledge, no entropy measurements for itaconates have previously been reported in the literature.

Experimental Section

Materials. Dicyclohexyl itaconate (DCHI) was prepared via the method of Velickovic[33] with the following modifications: After the reaction, the mixture was distilled twice under reduced pressure (1 mmHg). Between distillations the crude DCHI was dissolved in a minimal amount of chloroform and dripped slowly into *n*-hexane. The formed white solid was filtered off, and the *n*-hexane evaporated. The crude DCHI was subsequently dissolved in a minimal amount of chloroform again and percolated through a basic alumina column with chloroform as the solvent. The percolate was collected and placed on the high-vacuum line to remove the solvent, leaving a highly viscous colorless oil (for a detailed NMR characterization see ref 13). Dibutyl itaconate (DBI, Aldrich, 96%) was purified by percolating over a column of activated basic alumina. Dimethyl itaconate (DMI, Aldrich, 99% purity) was used as received. The photoinitiator 2,2-dimethoxy-2-phenylacetophenone (DMPA) (Aldrich, 99%) was used as received. Tetrahydrofuran (THF, Aldrich) for SEC measurements was refluxed over potassium, distilled, and stabilized with 2,6-di-*tert*-butyl-*p*-cresol. *N*-Methylformamide (Aldrich, 99%) and cyclohexanone (Ajax Chemicals, 99%) were used as received. The thermal initiator azobis(isobutyronitrile) (AIBN, Aldrich, 99%) was recrystallized twice from cyclohexane prior to use.

Polymerizations. All samples consisted of monomer or a monomer/solvent mixture (total volume 1.0 mL) with a photoinitiator concentration between 5×10^{-3} and 3.5×10^{-2} mol

L^{-1}. Prior to laser irradiation, all samples were thoroughly deoxygenated with a nitrogen stream for a period of 10 min. A Continuum Surelite I-20-Nd:YAG pulsed laser system was used to generate radiation bursts (20 ns) at a wavelength of 355 nm with a single pulse energy ranging between 15 and 30 mJ and a beam diameter of 6 mm. Care was taken to ensure a homogeneous intensity profile over the whole optical cross section. The applied laser pulse patterns were controlled with an external digital pulse generator (Quantum Composer 9412A and 9612 models). Isothermal reaction conditions were maintained using a recirculating bath including a feedback loop through a thermocouple attached to the side of the reaction cell. The experimental rig employed is very similar to the one described previously.[34] The bath fluid used was a 50:50 mix of ethylene glycol and water. The samples for the multipulse initiated PLP were irradiated with 4−20 repetitive bursts of 5−30 laser pulses (with pulse frequencies of 10 or 20 Hz), leading to an overall polymerization time of 0.33−6 min, depending on the individual dark time between bursts, t_0. The samples for conventional PLP were irradiated with single laser pulses of between 0.202 and 20 Hz with an overall polymerization time of 5−62 min. Cell design limits the study to atmospheric pressure; thus, the maximum temperature is determined by the normal boiling point of the monomer or the monomer/solution mixture. Monomer/solvent mixtures were prepared at room temperature (20 °C) on a molar basis, with monomer concentrations at the respective reaction temperatures calculated by assuming volume additivity[35] using pure component densities measured via an Anton Paar (5000) density meter. The complete collection molecular weight data obtained in the present study can be found in the Supporting Information section in Tables S1−S7.

Size Exclusion Chromatography. Chain length distributions (CLDs) for *p*DMI were measured via SEC on a Shimadzu modular LC system comprising a DGU-12A solvent degasser, a LC-10AT pump, a SIL-10AD autoinjector, a CTO-10A column oven, and a RID-10A refractive index detector. The system was equipped with a Polymer Laboratories 5.0 μm bead-size guard column (50 × 7.5 mm), followed by three linear PL columns (10^5, 10^4, and 10^3 Å). The eluent was THF at 40 °C with a flow rate of 1 mL min^{-1}. Calibration curves were generated using both poly(methyl methacrylate) and polystyrene standards in molecular weight ranges between 500 and 10^6 g mol^{-1}. The injection volume was 50 μL (5 mg mL^{-1}). SEC traces were evaluated using the Cirrus 1.0 software package (PL). The Mark−Houwink−Kuhn−Sakurada (MHKS) constants of polystyrene ($K = 14.1 \times 10^{-5}$ dL g^{-1} and $a = 0.70$)[36] and poly(methyl methacrylate) ($K = 12.8 \times 10^{-5}$ dL g^{-1}, $a = 0.697$)[37] were subsequently used to create a universal calibration curve which, in conjunction with the MHKS constants of *p*DMI (THF, $K = 46 \times 10^{-3}$ mL g^{-1}, $a = 0.510$), provided access to absolute molecular weight distributions for *p*DMI. CLDs for *p*DBI and *p*DCHI were determined using a similar SEC system with a column temperature of 25 °C. The Mark−Houwink−Kuhn−Sakurada (MHKS) constants of *p*styrene and *p*(methyl methacrylate) were then used to create a universal calibration curve which, in conjunction with the MHKS constants of *p*DCHI (THF (25 °C), $K = 23.3 \times 10^{-3}$ mL g^{-1}, $a = 0.580$), provided access to absolute molecular weight distributions. MHKS constants of *p*DBI (toluene (25 °C), $K = 5.7 \times 10^{-3}$ mL g^{-1}, $a = 0.70$) provided access to absolute molecular weight distributions for *p*DBI. There are currently no MHKS constants available for *p*DBI in THF. However, it has recently been demonstrated that those obtained in toluene can be used in THF systems.[38]

On-Line Fourier Transform−Near Infrared (FT-NIR) Spectroscopy. FT-NIR spectroscopy was employed to ensure that monomer to polymer conversions did not exceed 5% in each case. Monomer to polymer conversions were determined by transferring a portion of the irradiated (PLP) mixture after reaction into a 1 mm optical path length Infrasil cell (Starna Optical), and the decrease of the intensity of the first vinylic stretching overtone of the monomer at $\upsilon = 6166$ cm^{-1} (in the case of DCHI, with a slightly different υ_{max} value for DBI and DMI) compared to a nonreacted sample was determined. The FT-NIR measurements were performed using a Bruker IFS66\S Fourier transform spectrometer equipped with a tungsten halogen lamp, a CaF_2 beam splitter, and a liquid nitrogen cooled InSb detector. Each spectrum in the spectral region of 8000−4000 cm^{-1} was calculated from the coadded interferograms of 12 scans with a resolution of 2 cm^{-1}. For conversion determination, a linear baseline was selected between 6240 and 6120 cm^{-1}. The integrated absorbance between these two points was subsequently used to calculate the monomer-to-polymer conversion via Beer−Lambert's law. Other integration methods or methods using only the variation of the peak height at 6166 cm^{-1} have been tested in this study and yield identical results.

Table 1. Density/Temperature Relationships in the Temperature Range 20−90 °C for the Monomers and Solvents Employed in the Present Study

monomer/solvent	density function
DMI	d/g $mL^{-1} = 1.14265 - 0.00107T$
DBI	d/g $mL^{-1} = 1.00083 - 0.0009T$
DCHI[a]	d/g $mL^{-1} = 1.0751 - T \times 8.774 \times 10^{-4} + T^2 \times 5.940 \times 10^{-7}$
cyclohexanone	d/g $mL^{-1} = 0.966 - 0.0009T$
N-methylformamide	d/g $mL^{-1} = 1.0209 - 0.0009T$

[a] Density function determined previously.[13]

Differential Scanning Calorimetry (DSC). The heats of polymerization, ΔH, of DCHI and DBI in bulk were determined in duplicate experiments via on-line DSC. Monomer with AIBN (5×10^{-2} mol L^{-1}) was thoroughly deoxygenized via nitrogen purging and handled inside a glovebag filled with dry nitrogen gas. Exactly weighed amounts of solution (close to 70 mg) were loaded to aluminum pans that were sealed with aluminum lids. The polymerization heat was determined isothermally at 60 °C via measuring the heat flow vs an empty sample pan in a differential scanning calorimeter (Perkin-Elmer DSC 7 with a TAC 7/DX thermal analysis instrument controller). After completion of the reaction, the remaining monomer concentration was determined via FT-NIR spectrometry, by dissolving the entire contents of the DSC pan in a known quantity of tetrahydrofuran (THF) and subsequent comparison with a sample containing a known quantity of monomer and THF. The derived enthalpies are given (together with other parameters) in Table 2.

Solvent Selection. The selection of appropriate solvents for the present study of the depropagation kinetics of sterically hindered monomers is driven by two considerations: (i) the solvent needs to display a sufficiently high boiling point in order to investigate polymerizations at elevated temperatures ($T > 80$ °C); (ii) the solvent should not participate in transfer to solvent reactions to any noticeable extent, since these transfer processes interfere considerably with the PLP methodology. Although DBI undergoes intramolecular chain transfer reactions at elevated temperatures,[39] these reactions may be suppressed by the presence of amide compounds.[40] It has been suggested that it is primarily the hydrogen-bonding ability of the amide species with the itaconate moieties that suppress the possible intra- and intermolecular transfer reactions previously described. In addition, it has also been suggested that the bulkiness of the amide compound is one of the important factors in controlling the hydrogen-bonding interaction.[39,40] Thus, *N*-methylformamide was selected as solvent for DBI and DMI since it also has a sufficiently high boiling point ($T_b = 198$ °C). For the DCHI polymerization, cyclohexanone was selected as solvent, mainly driven by a low solvent to monomer transfer constant[41] and a high boiling point ($T_b = 153$ °C). The reason that cyclohexanone was used instead of *N*-methylformamide is associated with the significantly decreased likelihood of backbiting reactions occurring in DCHI systems as a result of the extremely large substituent groups of the DCHI monomer.

Monomer and Solvent Densities. The densities, d, necessary for the calculation of monomer concentration for each experiment were determined using a DMA 5000 density meter (Anton Paar) in the temperature range between 20 and 90 °C.

Table 2. Average Effective Propagation Rate Coefficients, k_p^{eff}, for Dicyclohexyl, Dibutyl, and Dimethyl Itaconate at Varying Reaction Temperatures and Initial Monomer Concentrations[a]

T/°C	$DCHI_{3.6M}^{bulk}$	$DCHI_{3.1M}$	$DCHI_{2.7M}$	$DCHI_{2.5M}$	$DCHI_{1.8M}$	$DBI_{4.1M}^{bulk}$	$DMI_{7.1M}^{bulk}$	$DMI_{3.1M}$
0	0.7					2.5	3.6	
10	1.2					3.8	5.1	
20	2.0[b]				1.2	5.4	8.4	
25	2.4[c]							
30	2.8[b]				1.7	7.1	12.0	
40	3.7[b]	3.1		2.5	2.2	8.8	17.5	15.0
50	4.7[c]	3.9	3.5	2.9	2.8	11.4	23.5	21.6
60	6.8	5.6	4.1	3.3	3.5	13.4	30.7	25.0
70	7.8	6.2	5.4	4.1	4.4	13.0	42.8	33.3
80	7.7	6.4	5.8			13.2	48.7	38.8
90	6.6	4.5				10.5	50.1	

[a] k_p^{eff} was calculated from the first point of inflection of the associated molecular weight distributions. Only those distributions that clearly displayed multiple overtones were used to derive k_p^{eff} values. The complete collation of the associated molecular weight data (L_1 to L_3) can be found in the Supporting Information Tables S1–S7. [b] Average of the data deduced in this study and previously reported[13] k_p^{eff} values. [c] Previously reported data.[13]

The best fit equations to the density data are collated in Table 1. The individually measured density vs temperature relationships can be found (alongside the best fit lines) in the Supporting Information (Figures S1–S4).

Simulations. All simulations of chain length distributions were carried out using the program package PREDICI (Polyreaction Distributions by Countable System Integration), version 5.36.3, on a Pentium M, 1.6 GHz Intel-IBM-compatible computer.

Results and Discussion

Experimental Results of Multipulse-Initiated PLP of Bulk DCHI. The monomer of greatest interest and with potentially the largest applicability of all the itaconate monomers studied in the present work is DCHI. DCHI is the largest and most sterically hindered of the monomers studied and appears to have the greatest radical stability due to its steric bulk. The ability to obtain well-resolved PLP distributions—well into a temperature region where depropagation can no longer be neglected—evidences the slow propagation rate of the monomeric species as well as free radical stability. Figure 1 depicts MWD's and derivative plots from PLP experiments at temperatures between 20 and 100 °C.

The multimodal distributions ($20 < T < 90$ °C) are typical of molecular weight distributions (MWDs) produced by PLP. Values of k_p^{eff} are calculated using eq 1 from the inflection point of the distribution determined from the maximum on the corresponding derivative plot. The increase in k_p^{eff} is typical of the normal increase caused by its Arrhenius temperature dependence up to 60 °C. However, beyond this temperature the increase of k_p^{eff} halts and subsequently drops as the temperature is further increased to 90 °C: depropagation has started to significantly affect k_p^{eff}. At 90 °C, L_1 falls back to a lower molecular weight; k_p^{eff} is almost the same as that determined at 60 °C. No k_p^{eff} information can be obtained from the PLP generated MWD at 100 °C (under a variety of conditions, including variations in the dark time, number of cycles, and laser intensity), which does not display any structure associated with pulsed laser control and is shifted to lower molecular weight values. This latter result suggests that 100 °C is approaching the ceiling temperature of the system: the rate of depropagation approaches that of propagation and the relative rate of chain transfer increases, resulting in a dramatic decrease in the average molecular weight and a loss of characteristic PLP features. The qualitative behavior illustrated in Figure 1 is captured quantitatively by transforming measured inflection points to k_p^{eff} values. Figure 2 depicts an Arrhenius plot of all of the k_p^{eff} data for bulk DCHI, including the low temperature (20–50 °C) results published previously.[13] The data are summarized in Table 2 together with the results from other systems under consideration in this study (see below).

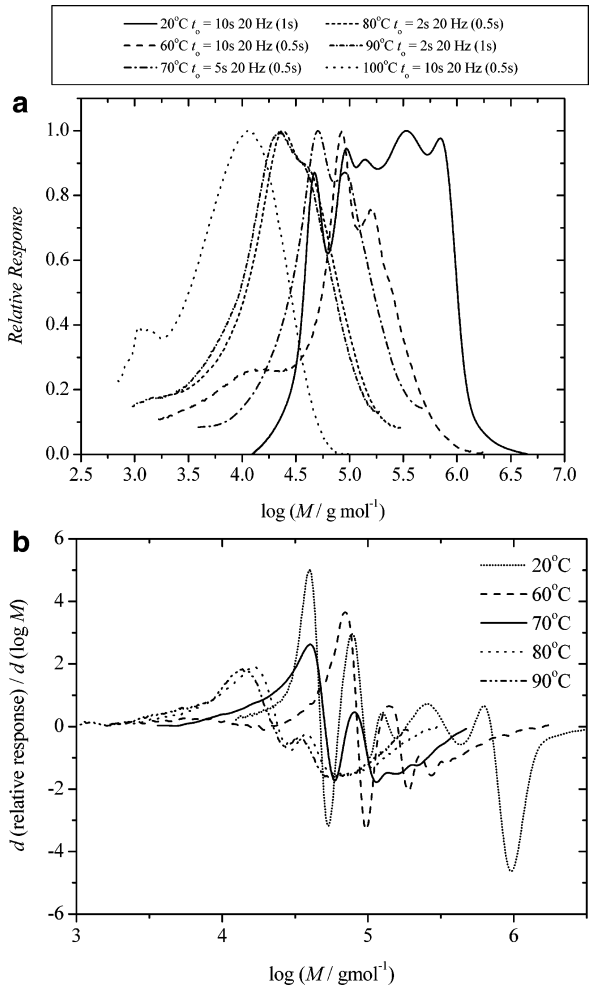

Figure 1. (a) Full molecular weight distributions generated via multipulse pulsed laser dicyclohexyl itaconate bulk free radical polymerization using 2,2-dimethoxy-2-phenylacetophenone as photoinitiator in the temperature range between 20 and 100 °C. (b) Corresponding first derivatives of the same molecular weight distributions from which the inflection points were collected to deduce the effective propagation rate coefficients, k_p^{eff}, listed in Table 2.

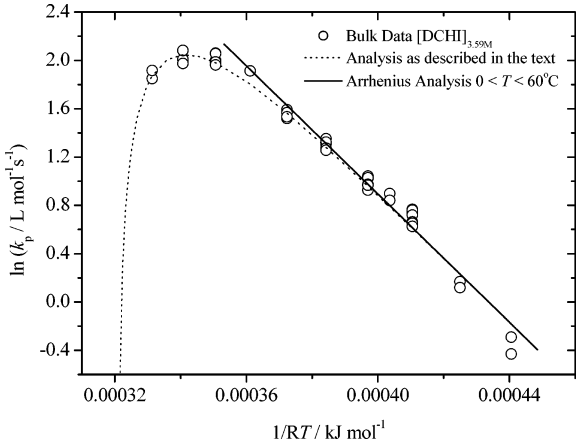

Figure 2. Experimental effective propagation rate coefficients, k_p^{eff}, obtained via multipulse pulsed laser polymerization for bulk dicyclohexyl itaconate free radical polymerization between 0 and 90 °C. The data have been analyzed by a conventional Arrhenius analysis (full line) for the forward propagation rate coefficient, k_p, in the temperature between 0 and 60 °C as well as via the methodology described in text (dotted line).

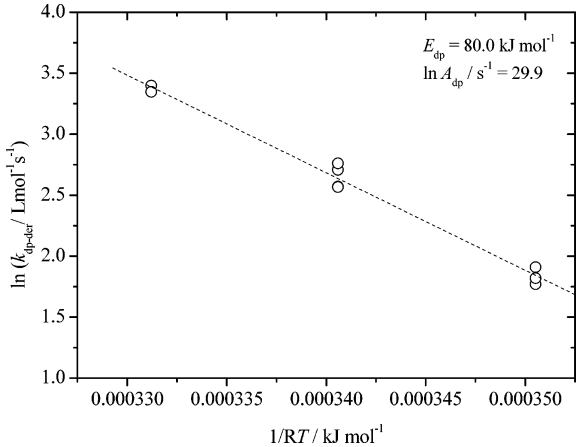

Figure 3. Depropagation rate coefficients, k_{dp}, obtained in dicyclohexyl itaconate bulk free radical polymerization as a function of reaction temperature (70 < T < 90 °C). The associated preexponential factor, A_{dp}, and activation energy, E_{dp}, of depropagation can also be found in Table 3.

The solution data—also presented in Table 2—are discussed later (see below). The straight line plotted in Figure 2 results from an Arrhenius fit to the (bulk) data collected at temperatures below 61 °C. The resulting Arrhenius parameters (in the temperature range between 0 < T < 60 °C) read E_p = 26.5 kJ mol^{-1} and ln A_p = 11.5 L mol^{-1} s^{-1}.[42] These numbers are relatively close to a similar data set reported in a slightly smaller temperature region (20 < T < 50 °C, E_p = 22.8 kJ mol^{-1} and ln A_p = 9.76 L mol^{-1} s^{-1}).[13] The extrapolation of the Arrhenius line in Figure 2 to higher temperatures clearly does not provide an adequate representation of the experimental data, which begins to deviate from k_p predictions at a temperature of 70 °C. The value of k_p^{eff} at 90 °C is 6.8 L mol^{-1} s^{-1}. This is a factor of 2.3 times lower than the extrapolated k_p value from the Arrhenius plot. Clearly, the effects of depropagation cannot be neglected at this temperature. An estimation method previously employed in a depolymerization study by Hutchinson et al.[18] has been used to estimate the parameters E_{dp} and A_{dp}, where estimates of k_{dp} are calculated for the data points collected in the region where depropagation is effective and cannot be neglected. A linearized fit is performed via eq 11 in the region of effective depolymerization (temperature range between 70 and 90 °C) where eq 12 is employed to determine values for k_{dp-der} (derived depropagation rate coefficient):

$$\ln(k_{dp-der}) = \ln(A_{dp}) - (E_{dp}/R)(1/T) \qquad (11)$$

$$k_{dp-der} = (k_{p-ext} - k_p^{eff})[M] \qquad (12)$$

where k_{p-ext} is calculated assuming the forward Arrhenius parameters (A_p and E_p) are valid over the entire temperature range. The linearized plot fitted to eq 11 is shown in Figure 3. The above analysis procedure yields numbers for activation parameters A_{dp} and E_{dp} for the depropagation reaction, i.e., ln A_{dp}/s^{-1} = 29.9 and E_{dp} = 80.0 kJ mol^{-1}. The values are very close to previously reported numbers in methacrylate systems.[18] From the complete set of the forward and reverse Arrhenius parameters, the polymerization enthalpy and entropy can be calculated via eqs 7 and 8: $\Delta H = -53.5$ kJ mol^{-1} and $\Delta S = -142.3$ J mol^{-1} K^{-1}. The above analysis is supported by an independent measurement of the enthalpy carried out via monitoring the heat of polymerization via isothermal differential scanning calorimetry (DSC, see Experimental Section), which returned a value of $\Delta H = -55.0$ kJ mol^{-1}. The completed parameter set for all monomers is collated in Table 3.

Effect of Depropagation on the Resulting Molecular Weight Distributions in Multipulse PLP of DCHI. It is mandatory to establish in a quantitative fashion why multipulse PLP fails to yield well-structured molecular weight distributions under conditions where propagation becomes prominent. For this purpose, a relatively simple kinetic scheme was implemented into the PREDICI program package comprising pulsed initiation, propagation, depropagation, and bimolecular termination. The simulation returned the full molecular weight distributions, which were subsequently subjected to an algorithm which introduced SEC broadening (σ(log M) = 0.05). Finally, the distributions were analyzed analogous to the experimental distributions to yield the effective rate coefficient of depropagation, k_p^{eff}. The rationale behind the simulations was as follows: A reaction condition (i.e., multipulse sequence) was selected at which a well-structured MWD resulted under actual experimental conditions at a temperature where depropagation reactions are nondominating. The simulation was carried out and—not surprisingly—the initial input value for k_p was returned upon analysis of the MWD. Subsequently, the simulation was repeated, this time however with a nonzero value for the rate coefficient of depropagation. In a stepwise fashion, the depropagation rate coefficient was increased and the resulting effect on the MWD observed. The simulation was carried out for a reaction temperature of 20 °C, for which the following rate coefficient values are valid: k_p = 2.04 L mol^{-1} s^{-1}, k_{dp} (see Figure 4), $k_{t,d}$ = 147 L mol^{-1}s^{-1}, $k_{t,c}$ = 49 L mol^{-1} s^{-1} (indices "d" and "c" correspond to disproportionation and combination with 25% of termination by combination),[13] k_i = 20.4 L mol^{-1} s^{-1}, and primary radical termination k_t^p = 10^6 L mol^{-1} s^{-1}.[12] The rate coefficient of depropagation was varied between 0 and 6 s^{-1}. For the simulations a primary free radical concentration generated by each

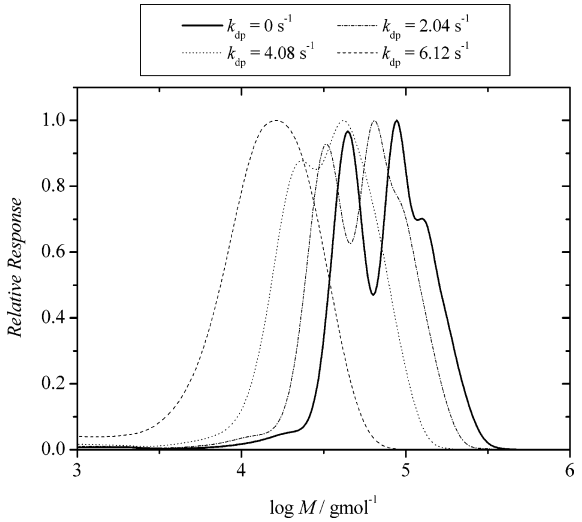

Figure 4. Calculated full molecular weight distributions (via PREDICI) resulting from multipulse pulsed laser polymerization (PLP) experiments of bulk dicyclohexyl itaconate. The simulation assumes a range of values for the depropagation rate coefficient, k_{dp}, and examines its effect on the applicability of the PLP method (for details, including the simulation input parameters, see text).

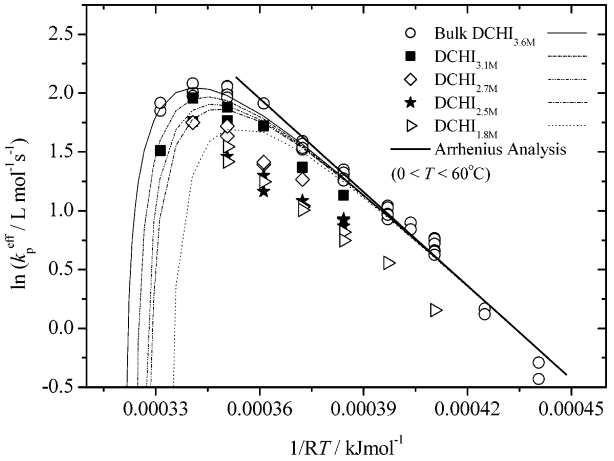

Figure 5. Experimental effective propagation rate coefficients, k_p^{eff}, obtained via multipulse pulsed laser polymerization for dicyclohexyl itaconate in solution (cyclohexanone) free radical polymerization between 20 and 90 °C. The polymerizations were carried out with varying mol % of solvent as indicted within the figure. The bulk data have been analyzed by a conventional Arrhenius analysis (thick full line) for the forward propagation rate coefficient, k_p, as well as via the methodology described in text (thin full line), and the resulting activation parameters have been used to model the solvent experiments.

laser pulse of 3×10^{-6} mol L^{-1} was assumed. The pulse pattern was composed of a 20 Hz burst of 1 s, followed by a dark time period 9 s.

Inspection of Figure 4 clearly demonstrates that, with increasing proportions of depropagation present in the reaction sequence, the obtained molecular weight distributions lose their structural distinctions. At a depropagation level of $k_{dp} = 2$ s^{-1} a clear PLP structure can be detected in the molecular weight distribution, while at a depropagation level of 4 s^{-1} the PLP structure is clearly starting to disappear. At a depropagation level of 6 s^{-1}, no PLP structure is observable. We also evaluated other multipulse burst patterns in the simulations, and it comes at no surprise that a change in the multipulse burst pattern does not allow for obtaining well-structured PLP distributions under strong depropagation influences. These findings are in complete agreement with the corresponding experimental data, where we could not identify PLP conditions that allowed for the generation of well-structured and self-consistent (i.e., having overtones) molecular weight distributions under strong depropagation conditions. Thus, the experimental observation that no PLP distribution can be obtained beyond certain temperatures, coupled with the nonlinear Arrhenius relationships, provides evidence that depropagation becomes prominent. At first sight, it comes at some surprise that no PLP structures can be observed at an effective k_p in the depropagation region, whereas a clear distribution can be observed an identical effective k_p at lower temperatures. Certainly one of the underpinning reasons for this behavior is associated with a broadening effect in the chain lengths of the propagating radical population due to the larger number of propagation (and depropagation) events that occur during each dark time interval. It is worthwhile to test whether the numbers determined for the DCHI bulk system for k_p and k_{dp} describe the actual experimentally determined molecular weight distributions. We simulated the molecular weight distributions for 30 and 80 °C (i.e., in the nondepropagation and depropagation regimes) and compared the simulation output with the experimental data. Not surprisingly, the agreement between the simulated and modeled distributions is good (see Figure S5 in the Supporting Information as well as the caption to this figure for the modeling parameters). It should be kept in mind when comparing the experimental and simulation output that there is unavoidably a degree of uncertainty about the magnitude of the actual radical concentration generated per single laser pulse and the ratio of combination to disproportionation. Thus, although correct values for the kinetic rate coefficients were employed, the actual peak heights of the simulated distributions can differ from those observed experimentally. The situation could be improved via a distribution data fitting procedure. However, we do not wish to embark on such an exercise, which is beyond the scope of the present study (please see ref 43 for a good example on PLP distribution fitting and optimization).

Experimental Results of Multipulse-Initiated PLP of DCHI in Solution. Equation 6 indicates that the relative importance of depropagation is inversely proportional to the monomer concentration and in fact increases as the monomer concentration is decreased. It can thus be anticipated that as the monomer concentration decreases, the k_p^{eff} values determined will deviate from k_p at lower temperatures. Experiments were thus conducted to determine k_p^{eff} with 85, 75, 70, and 50 mol % of $[DCHI]_{bulk}$ (using cyclohexanone as the solvent). Figure 5 shows the data obtained at these monomer concentrations as well as a theoretical description for k_p^{eff} using the activation parameters determined from the DCHI bulk systems (i.e., A_p, E_p, A_{dp}, and E_{dp}). The theoretically expected k_p^{eff} values were thus obtained by using eqs 7−12 under variation of the monomer concentration. The results are also collated in Table 2.

Inspection of Figure 5 indicates indeed that with increasing solvent concentration it becomes increasingly difficult to obtain structured molecular weight distributions that allow for the extraction of k_p^{eff} values at higher temperatures. Only at the lowest solvent concentration (closed squares) was it possible to obtain a

k_p^{eff} value in the depropagation region. At the next highest concentration (open diamonds) it can just be seen that the k_p^{eff} levels off. For the two highest concentrations, we could not identify PLP−SEC conditions that lead to structured molecular weight distributions. However, this observation in itself suggests that depropagation becomes more pronounced at lower temperatures as the solvent concentration is increased. As the simulated k_p^{eff} curves in Figure 5 demonstrate, the effect of solvent addition on k_p^{eff} is relatively small (e.g., at 70 °C the k_p^{eff} for the highest solvent concentration is reduced by approximately 25%). If one considers that the determined k_p^{eff} values are beset with an error of between ±20 and ±30% (a value which is the generally accepted accuracy of PLP−SEC based k_p determination, see for example the IUPAC PLP−SEC benchmark paper on styrene[16]), the expected effects almost lie within this error range. Inspection of Figure 5 also shows that, with increasing concentration of the solvent, there tends to be a general lowering of k_p^{eff}, which is also observed in the temperature region where there should be no depropagation. The simulated k_p^{eff} curves show a quantitative mismatch between the predictions and the experimental data. Decreasing the monomer concentration at elevated temperatures leads to a lower value of k_p^{eff} than expected. Such a deviation was also noted in the early study of the depolymerization kinetics of *n*-dodecyl methacylate by Hutchinson et al.[18] and the literature cited therein.[44−46] It is not unreasonable to attribute this mismatch to a solvent effect on k_p^{eff}. The mismatch becomes more pronounced as the monomer concentration is decreased, with a k_p^{eff} in 50 mol % solution approximately 50% lower than that in bulk (see Figure 5 in the low-temperature region).

Experimental Results of Multipulse-Initiated PLP of DBI in Bulk and Solution. If DBI is of less steric bulk than DCHI, one would expect that its ceiling temperature is somewhat higher. Electronically, both DBI and DCHI are very similar, and thus the activation energies of the propagation reaction observed for DBI and DCHI should be very similar, but there should be a pronounced difference in the preexponential factor due to steric reasons. Surprisingly, there is a difference in both the preexponential factor (decreasing from $\ln A_p$/L mol^{-1} s^{-1} = 11.5 to $\ln A_p$/L mol^{-1} s^{-1} = 10.4) and—very pronounced—the activation energy. The Arrhenius analysis of the data depicted in Figure 6 in the temperature range between 0 and 50 °C returns an activation energy for the propagation reaction of close to 21.3 kJ mol^{-1}. This number is in good agreement with a previously reported value of 19.4 kJ mol^{-1} for the same quantity.[47] While it cannot be excluded that the absolute values of the propagation rate coefficient are somewhat affected (and thus the derived number for A_p) by the use of Mark−Houwink−Kuhn−Sakurada (MHKS) parameter valid for toluene in THF solution (although the effects should be minor), it is even more unlikely that their relative position and thus the activation energy is affected. It has been demonstrated in an earlier—smaller temperature range—study on DMI that the use of various Mark−Houwink parameters does indeed not effect the observed activation energy.[14]

In the high-temperature regime (at temperatures exceeding 60 °C), the data depicted in Figure 6 demonstrate that the effective rate coefficient of depropagation does not further increase as predicted by the Arrhenius relationship for the forward reaction, thus indicating

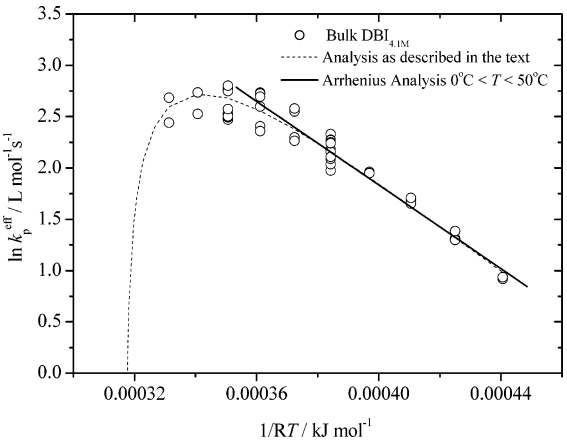

Figure 6. Experimental effective propagation rate coefficients, k_p^{eff}, obtained via multipulse and conventional pulsed laser polymerization in bulk dibutyl itaconate free radical polymerization between 0 and 90 °C. The data have been analyzed by a conventional Arrhenius analysis (full line) for the forward propagation rate coefficient, k_p, as well as via the methodology described in text (dotted line).

the onset of depropagation. Similarly to the experiments carried out with DCHI, we attempted to obtain effective propagation rate coefficients for DBI in solution at temperatures exceeding 70 °C. However, it was not possible to identify any PLP conditions under which structured molecular weight distributions could be obtained. Such an observation may by itself suggest that depropagation becomes more pronounced at higher temperatures as the solvent concentration is increased (as pointed out in the DCHI section as well). However, it also should also be noted that there has been a detailed study of DBI free radical polymerization with regard to possible backbiting and transfer to polymer reactions in these systems.[40] Within this study it has been shown that the stereochemistry of the generated *p*DBI depends on the polymerization temperature. Polymers with a wide range of tacticities, from syndiotactic to isotactic-rich, can be obtained, which has been demonstrated by ^{13}C NMR spectroscopy. The same study reported that DBI undergoes intramolecular chain transfer reactions at elevated temperatures, which can (at least partly) be suppressed by the addition of amides to the reaction mixture (see the above section on solvent selection). It cannot be excluded that the tendency of DBI to from midchain radicals influences its suitability for PLP−SEC experiments.

To further investigate the change in activation energy when going from DCHI to DBI, the heat of polymerization, ΔH, was determined by on-line DSC and was close to −42.0 kJ mol^{-1}. The effective propagation rate data was subsequently analyzed by eqs 7−12 in order to arrive at the activation entropy (which is equivalent to deducing the value for A_{dp}), which is possible because all other parameters of the system are known (i.e., E_p, A_p, and ΔH plus the effective propagation rate coefficients k_p^{eff} as a function of temperature). In effect, a parameter optimization is carried out to determine the value ΔS such that eq 8 yields an optimum fit for the temperature-dependent effective propagation rate data. The value deduced for ΔS is −110 J mol^{-1} K^{-1}, considerably lower than the corresponding number for DCHI (−142 J mol^{-1} K^{-1}) and DMI (see below, −156 J mol^{-1} K^{-1}).[42] The low entropy is an indication that the system undergoes a lesser decrease in loss of freedom than both DCHI and DMI. Interestingly, both *p*DCHI and *p*DMI

Table 3. Activation Energies and Preexponential Factors for the Propagation and Depropagation Reaction of Dicyclohexyl, Dibutyl, and Dimethyl Itaconate as Well as Heats and Entropies of the Polymerization Processes (for Details See Text)

monomer	$\ln A_p$	E_p/kJ mol^{-1}	$[M]_0$/mol L^{-1}	$\ln A_{dp}$	E_{dp}/kJ mol^{-1}	$-\Delta H$/kJ mol^{-1}	$-\Delta S$/J mol^{-1} K^{-1}	T_c/°C
DMI	13.5	27.8	7.1	34.2	88.3	60.5[b]	156	114
DBI	10.4	21.3/19.4[c]	4.1	25.0	63.3	42.0[a]	110	109
DCHI	11.5	26.5	3.6	29.9	80.0	53.5/55.0[a]	142	114

[a] Value measured by on-line DSC in the current study. [b] Value deduced in an earlier calorimetry study.[32] [c] Value determined by Popovic et al.[47]

prepared under the PLP−SEC conditions of the present study precipitate very well in methanol at room temperature, whereas *p*DBI does not (it only precipitates at much lower temperature, $T < -20$ °C, in the same solvent). As inspection of Table 3 indicates, DBI is thus considerably different to both DCHI and DMI in terms of its thermodynamic and the related activation parameters. Significant differences in activation energy for monomers belonging to the same family—where no such differences would be expected—have been observed before. Of particular note is a pulsed laser study into the effects of the ester side chain on the propagation kinetics of alkyl methacrylates.[48] In there, it was found that all studied methacrylates displayed activation energies of close to 24 kJ mol^{-1}, with the only exception being dodecyl methacrylate (DMA), which showed an activation energy of close to 21 kJ mol^{-1}.[49] Prima facie, this discrepancy is as puzzling as the one reported in the present study. Given the distance between the ester side chain and the propagating center (corroborated by a lack of conjugation), one would expect that the ester side chain does not significantly affect the activation energy in both cases. In the case of DMA, the discrepancy was explained by assuming that the ester chain is coiled and part of it could lie relatively near the propagating radical chain end. Under such circumstances, the activation energy could be affected by through space interactions between the alkyl chain and the unpaired electron. In the case of DBI, one could potentially envisage a similar scenario leading to the same effect, especially because DBI carries two mobile ester side chains. In the case of DCHI, one would expect less interaction of the ester group with the radical center due the inflexibility of the ester group imparted by its cyclic nature.

Experimental Results of Multipulse-Initiated PLP of DMI in Bulk and Solution. The least sterically demanding monomer considered in the present study is DMI. DMI has been studied—albeit in a limited temperature range—previously via PLP−SEC. In here, we extend this initial data set to higher and lower temperatures and solution polymerization. On the basis of steric grounds alone, one would expect that DMI has the highest ceiling temperature and an activation energy for the forward reaction in line with the number reported for DCHI. Further, it may be anticipated that DMI displays the largest preexponential factor, A_p, of the three monomers. Indeed, inspection of Table 3 largely confirms these expectations. The preexponential factor is indeed a factor of ≈7 times larger than that recorded for DCHI, and the activation energies are (within experimental error) identical (27.8 vs 26.5 kJ mol^{-1}).

Figure 7 shows the dependence of the effective propagation rate coefficient on the temperature in both bulk and 50 mol % solution. Inspection of the figure clearly shows that at temperatures exceeding 70 °C the bulk polymerization process does not adhere to the Arrhenius relationship anymore. At 50 mol % solvent in the reaction mixture, the decrease is not pronounced. However, a slight effect of the solvent on the propagation rate coefficient—similar to that observed in the case of DCHI—can be observed. The data were analyzed using an independently determined value for heat of polymerization, $\Delta H = -60.5$ kJ mol^{-1},[32] and the activation parameters obtained for the forward propagation reaction in the temperature range between 0 and 70 °C ($E_p = 27.8$ kJ mol^{-1}, $\ln A_p$/L mol^{-1} s^{-1} = 13.5) in an identical fashion as described above for DBI. The analysis procedure returned a value for the entropy of polymerization, ΔS, of -156 J mol^{-1} K^{-1}.[42] This number is similar to the value deduced in DCHI polymerization for the same parameter ($\Delta S^{DCHI} = -142$ J mol^{-1} K^{-1}) but departs markedly from the number obtained for DBI (see above; $\Delta S^{DBI} = -110$ J mol^{-1} K^{-1}). In addition, DMI displays the largest value for the preexponential factor of all three monomers, which is associated with the fact that it has the least steric bulk, and thus the frequency of successful collisions is considerably higher than in the case of DBI and DCHI. The dotted line in Figure 7 gives the temperature dependency of k_p^{eff} associated with the thermodynamic data collated in Table 3. As mentioned above, the excellent fit of the data with the measured data points is not surprising, since the dotted line is effectively the outcome of a fit procedure. It is noteworthy that the determined set of Arrhenius data for DMI bulk polymerization describes the temperature dependent solution data very well (dashed line in Figure 7) simply by adjusting the monomer concentration. The trend already observed for DCHI that the k_p^{eff} decreases

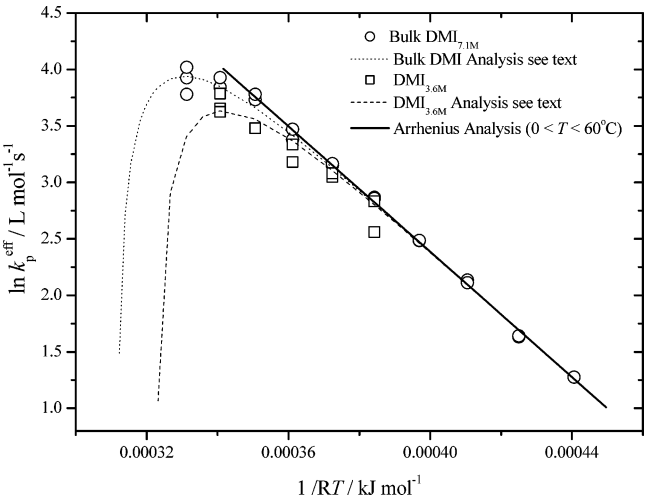

Figure 7. Experimental effective propagation rate coefficients, k_p^{eff}, obtained via conventional pulsed laser polymerization for dimethyl itaconate in bulk and solution (*N*-methylformamide, see text) free radical polymerization between 0 and 90 °C. The data have been analyzed by a conventional Arrhenius analysis (full line) for the forward propagation rate coefficient, k_p, as well as via the methodology described in text (broken lines).

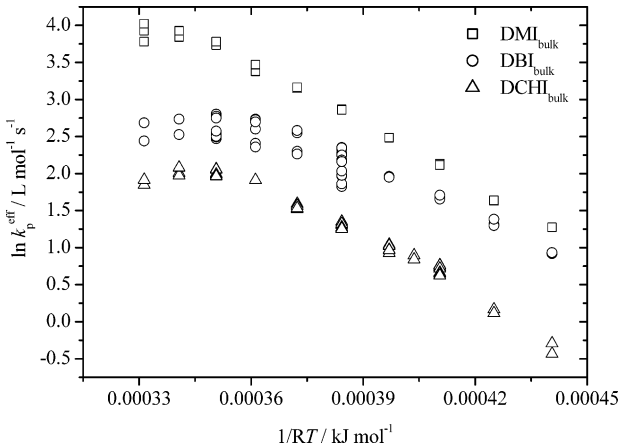

Figure 8. Effective propagation rate coefficients, k_p^{eff}, for dicyclohexyl, dibutyl, and dimethyl itaconate as a function of temperature measured via conventional and multipulse PLP–SEC in bulk.

at an identical temperature with increasing amounts of solvent (i.e., the polymer depropagates at lower temperatures) is also found for DMI.

The thermodynamic data collated in Table 3 can be employed to calculate the ceiling temperature. Inspection of Table 3 shows that DMI and DCHI as well as DBI have ceiling temperatures very close to each other in the range of 110 °C. The ceiling temperature for the hindered monomers of the present study thus lies considerably lower than those observed for *p*styrene (T_c = 310 °C)[9] and *p*(methyl methacrylate) (T_c = 220 °C),[50] but also significantly higher than α-methylstyrene (T_c = 61 °C).[51] The monomers studied in the present contribution thus represent a compromise between relatively good polymerizability at nondemanding reaction conditions, while at the same time opening an avenue to depolymerize the generated material at a later stage in applications such as macromolecular imprinting.

Conclusions

In the present study we have presented effective propagation rate coefficient data, k_p^{eff}, for three sterically hindered monomers in wide temperature ranges as well as in both bulk and solvent systems. The present data demonstrate that the stercially hindered monomers DCHI, DBI, and DMI display relatively low ceiling temperatures (see Figure 8 for a direct comparison of the bulk propagation rate coefficients at various temperatures), evidenced by the deviation of the observed effective rate coefficient of propagation, k_p^{eff}, from the low-temperature regime Arrhenius analysis.

The data obtained for DCHI allowed for an estimation of the entropy and enthalpy of polymerization in bulk directly from the temperature dependent k_p^{eff} data. In addition, the polymerization enthalpy was also determined via on-line DSC. For DBI bulk polymerization, the heat of polymerization was measured only via differential scanning calorimetry (a literature value is available for DMI)[32] and employed in conjunction with the propagation rate data to deduce the polymerization entropy for both monomers. Surprisingly, DBI displays a very different behavior when compared to DMI and DCHI, showing a significantly lower activation energy for the forward reaction and heat of polymerization accompanied by a relatively high entropy of polymerization. With increasing amounts of solvent in the reaction mixture, it is increasingly more difficult to obtain structured molecular weight distributions that allow for the deduction of effective propagation rate coefficients at temperatures where depropagation is significant. However, this observation may in itself be an indication that depropagation becomes more prominent at lower reaction temperatures with decreasing monomer concentration. Further, the addition of a solvent leads to a significant decrease of the effective propagation rate coefficients also in the low-temperature regimes in the case of DCHI polymerizations. The data gathered in the present contribution will serve as an important piece of information in guiding material design based on depolymerization methodologies. In addition, the data are invaluable in judging the potential applicability of RAFT-based methodologies toward obtaining chain length dependent termination rate coefficients in these systems.

Acknowledgment. C.B.-K., M.H.S., and T.P.D. acknowledge financial support from the Australian Research Council (ARC) in the form of two Discovery grants related to this project. Z.S. acknowledges a PhD scholarship from the Faculty of Engineering (UNSW). T.P.D. acknowledges the receipt of an Australian Professorial Fellowship (ARC). The authors thank Dr. Philipp Vana for initial help with the multipulse experiments as well as Dr. Alexander Theis for his help with the DSC experiments. Further, the authors thank Mr. Istvan Jacenyik for his management of CAMD.

Supporting Information Available: Temperature–density relationship for the monomers and solvents as well as the complete molecular weight data (L_1 to L_3) alongside the respective experimental conditions. This material is available free of charge via the Internet at http://pubs.acs.org.

References and Notes

(1) (a) Mayadunne, R. T. A.; Rizzardo, E.; Chiefari, J.; Chong, Y. K.; Moad, G.; Thang, S. H. *Macromolecules* **1999**, *32*, 6977–6980. (b) Chiefari, J.; Mayadunne, R. T. A.; Moad, C. L.; Moad, G.; Rizzardo, E.; Postma, A.; Skidmore, A.; Thang, S. H. *Macromolecules* **2003**, *36*, 2273–2283. (c) Moad, G.; Chiefari, J.; Mayadunne, R. T. A.; Moad, C. L.; Postma, A.; Rizzardo, E.; Thang, S. H. *Macromol. Symp.* **2002**, *182*, 65–80. (d) Moad, G.; Chiefari, J.; Chong, Y. K.; Krstina, J.; Mayadunne, R. T. A.; Postma, A.; Rizzardo, E.; Thang, S. H. *Polym. Int.* **2000**, *49*, 993–1001.

(2) Szablan, Z.; Ah Toy, A.; Davis, T. P.; Hao, X.; Stenzel, M. H.; Barner-Kowollik, C. *J. Polym. Sci., Polym. Chem.* **2004**, *42*, 2432–2444.

(3) Matsumoto, A.; Sano, Y.; Yoshioka, M.; Otsu, T. *J. Polym. Sci., Polym. Chem.* **1996**, *34*, 291–299.

(4) Kobatake, S.; Yamada, B. *Macromol. Chem. Phys.* **1997**, *198*, 2825–2537.

(5) Kobatake, S.; Yamada, B. *Macromolecules* **1995**, *28*, 4047–4054.

(6) Kobatake, S.; Yamada, B. *J. Polym. Sci., Polym. Chem.* **1996**, *34*, 95108–.

(7) Matsumoto, A.; Yamagishi, K.; Otsu, T. *Eur. Polym. J.* **1995**, *31*, 121–124.

(8) Otsu, T.; Minai, H.; Toyoda, N.; Yasuhara, T. *Makromol. Chem.* **1985**, *12*, 133–142.

(9) Dainton, F. S.; Ivin, K. J. *Nature (London)* **1948**, *162*, 705–707.

(10) Kowollik, C. Ph.D. Thesis, Göttingen 1999, ISBN 3-89712-705-9.

(11) Buback, M.; Kurz, C. H.; Schmaltz, C. *Macromol. Chem. Phys.* **1998**, *199*, 1721–1727.

(12) Vana, P.; Yee, L. H.; Barner-Kowollik, C.; Heuts, J. P. A.; Davis, T. P. *Macromolecules* **2002**, *35*, 1651–1657.

(13) Vana, P.; Yee, L. H.; Davis, T. P. *Macromolecules* **2002**, *35*, 3008–3016.

(14) Yee, L. H.; Coote, M. L.; Chaplin, R. P.; Davis, T. P. *J. Polym. Sci., Polym. Chem.* **2000**, *38*, 2192−2200.
(15) Olaj, O. F.; Bitai, I.; Hinkelmann, F. *Makromol. Chem.* **1987**, *188*, 1689−1702.
(16) Buback, M.; Gilbert, R. G.; Hutchinson, R. A.; Klumperman, B.; Kuchta, F.-D.; Manders, B. G.; O'Driscoll, K. F.; Russell, G. T.; Schweer, J. *Macromol. Chem. Phys.* **1995**, *196*, 3267−3280.
(17) Yee, L. H.; Heuts, J. P. A.; Davis, T. P. *Macromolecules* **2001**, *34*, 3581−3586.
(18) Hutchinson, R. A.; Paquet, D. A.; Beuermann, S.; McMinn, J. *Ind. Eng. Chem. Res.* **1998**, *37*, 3567−3574.
(19) Kilroe, J. G.; Weale, K. E. *J. Chem. Soc.* **1960**, 3849−3854.
(20) Kukulj, D.; Davis, T. P. *Macromolecules* **1998**, *31*, 5668−5680.
(21) Vana, P.; Davis, T. P.; Barner-Kowollik, C. *Macromol. Rapid Commun.* **2002**, *23*, 952−956.
(22) Feldermann, A.; Stenzel, M. H.; Davis, T. P.; Vana, P.; Barner-Kowollik, C. *Macromolecules* **2004**, *37*, 2404−2410.
(23) Theis, A.; Feldermann, A.; Charton, N.; Stenzel, M. H.; Davis, T. P.; Barner-Kowollik, C. *Macromolecules* **2005**, *38*, 2595−2605.
(24) The term "ceiling temperature", T_c, does not seem to be universally defined. Since the T_c is associated with the monomer concentration for thermodynamic reasons, there seems to be some confusion with regard to the monomer concentrations for which T_c should be reported. While some studies reference T_c with regard to the bulk monomer concentrations, others use a 1 M monomer solution as reference state. The present study uses bulk monomer concentrations as reference when discussing ceiling temperatures.
(25) Hutchinson, R. A.; Aronson, M. T.; Richards, J. R. *Macromolecules* **1993**, *26*, 6410−6415.
(26) Beuermann, S.; Buback, M.; Davis, T. P.; Gilbert, R. G.; Hutchinson, R. A.; Klumpermann, B.; Olaj, O. F.; Russell, G. T.; Schweer, J. *Macromol. Chem. Phys.* **1997**, *198*, 1545−1560.
(27) Kornherr, A.; Zifferer, G.; Olaj, O. F. *Macromol. Theory Simul.* **1999**, *8*, 260−271.
(28) Barner-Kowollik, C.; Vana, P.; Davis, T. P. The Kinetics of Free-Radical Polymerization. In *Handbook of Radical Polymerization*; Davis, T. P., Matyjaszewski, K., Eds.; Wiley-Interscience: New York, 2002; p 187.
(29) Olaj, O. F.; Zifferer, G. *Makromol. Chem. Theory Simul.* **1992**, *1*, 71−90.
(30) Barner-Kowollik, C.; Davis, T. P. *Macromol. Theory Simul.* **2001**, *10*, 255−261.
(31) Busfield, W. K. In *Polymer Handbook*, 3rd ed.; Brandrup, J., Immergut, E. H., Eds.; Wiley-Interscience: New York, 1989; pp II, 363.
(32) Dainton, F. S.; Ivin, K. J.; Walmsmey, D. A. G. *Trans. Faraday Soc.* **1960**, *56*, 1784−1792.
(33) Velickovic, J.; Coseva, S.; Fort, R. J. *Eur. Polym. J.* **1975**, *11*, 377−380.
(34) Davis, T. P.; O'Driscoll, K. F.; Piton, M. C.; Winnik, M. A. *Macromolecules* **1992**, *22*, 2785−2788.
(35) The validity of volume additivity was verified by measuring the density of mixtures of DCHI/cyclohexanone (50:50 vol %) and DBI/*N*-methylformamide (50:50 vol %) at 30, 50, and 70 °C. The monomer concentrations derived under the assumption of volume additivity deviate by a maximum of 2% from the true monomer concentrations (i.e., $c_{DBI}^{30\ °C}$(assuming additivity) = 2.0183 mol L^{-1}, $c_{DBI}^{30\ °C}$ (using measured mixture densities)=2.0197 mol L^{-1} and (at 70 °C) $c_{DBI}^{70\ °C}$(assuming additivity) = 1.945 mol L^{-1}, $c_{DBI}^{70\ °C}$(using measured mixture densities) = 1.947 mol L^{-1}). A similar result was found for the DCHI/cyclohexanone system (i.e., $c_{DCHI}^{30\ °C}$(assuming additivity) = 1.786 mol L^{-1}, $c_{DCHI}^{30\ °C}$ (using measured mixture densities) = 1.8225 mol L^{-1} and (at 70 °C) $c_{DCHI}^{70\ °C}$ (assuming additivity) = 1.724 mol L^{-1}, $c_{DCHI}^{70\ °C}$ (using measured mixture densities) = 1.754 mol L^{-1}).
(36) Strazielle, C.; Benoit, H.; Vogl, O. *Eur. Polym. J.* **1978**, *14*, 331−334.
(37) Rudin, A.; Hoegy, H. L. W. *J. Polym. Sci., Part A1* **1972**, *10*, 217−235.
(38) Buback, M.; Egorov, M.; Junkers, T.; Panchenko, E. *Macromol. Chem. Phys.* **2005**, *3*, 333−341.
(39) Hirano, T.; Higashi, K.; Seno, M.; Sato, T. *J. Polym. Sci., Polym. Chem.* **2003**, *41*, 3463−3467.
(40) Hirano, T.; Tateiwa, S.; Seno, M.; Sato, T. *J. Polym. Sci., Polym. Chem.* **2000**, *38*, 2487−2491.
(41) Typical transfer constants for aliphatic ketones are around 1×10^{-5} mol L^{-1}. See for example: Chadha, R. N.; Shukla, J. S.; Mistra, G. S. *Trans. Faraday Soc.* **1957**, *53*, 240−246.
(42) The errors of the forward activation energies are estimated to not exceed ±3 kJ mol^{-1}. The errors of the heats of polymerization—determined via on-line DSC—are estimated to be no more than ±4 kJ mol^{-1}. If the point values for the reported ΔH values are employed to deduce ΔS, then the reported entropies are beset with an error of no more than ±4 J mol^{-1} K^{-1}. If the full range of error in ΔH is considered, the entropy error is larger and close to ±10 J mol^{-1} K^{-1}. Accordingly, the errors in the activation energy for the depropagation reaction are somewhat higher than those estimated for the forward process (±5 kJ mol^{-1}) when employing the procedure of fitting the entire $k_p^{eff}(T)$ function (as carried out for DMI and DBI). When determining E_{dp} via a direct Arrhenius plot (as performed for DCHI, Figure 3), its error is identical to that for the forward reaction, i.e., ±3 kJ mol^{-1}.
(43) Buback, M.; Busch, M.; Laemmel, R. A. *Macromol. Theory Simul.* **1996**, *5*, 845−861.
(44) O'Driscoll, K. F.; Monteiro, M. J.; Klumperman, B. *J. Polym. Sci., Polym. Chem.* **1997**, *35*, 515−520.
(45) Zammit, M.; Davis, T. P.; Willett, G. D.; O'Driscoll, K. *J. Polym. Sci., Polym. Chem.* **1997**, *35*, 2311−2321.
(46) Beuermann, S.; Buback, M.; Kuchta, F.-D.; Schmaltz, C. *Macromol. Chem. Phys.* **1998**, *199*, 1209−1216.
(47) Popovic, I. G.; Beuermann, S.; Buback, M. Proceedings 3rd IUPAC sponsored Symposium on Free Radical Polymerization: Kinetics and Mechanism, 2001.
(48) Zammit, M. D.; Coote, M. L.; Davis, T. P.; Willett, G. D. *Macromolecules* **1998**, *31*, 955−963.
(49) Hutchison, R. A.; Beuermann, S.; Paquet, D. A., Jr.; McMinn, J. H. *Macromolecules* **1997**, *30*, 3490−3493. Davis, T. P.; O'Driscoll, K. F.; Piton, M. C.; Winnik, M. A. *Macromolecules* **1990**, *23*, 2113−2119.
(50) Cook, R. E.; Dainton, F. S.; Ivin, K. J. *J. Polym. Sci.* **1958**, *29*, 549−556.
(51) McCormick, H. W. *J. Polym. Sci.* **1957**, *25*, 488−490.

MA050444L